DALTON
FULL PAPER

Iron(II) phosphonates: a new series of molecule-based weak ferromagnets †

Angela Altomare,[a] Carlo Bellitto,*[b] Said A. Ibrahim,[c] Mohammed R. Mahmoud[c] and Rosanna Rizzi[a]

[a] *CNR-Istituto di Ricerca per lo Sviluppo di Metodologie Cristallografiche, c/o Dipartimento Geomineralogico, Università di Bari, Via Orabona 4, Campus Universitario, I-70125 Bari, Italy*
[b] *CNR-Istituto di Chimica dei Materiali, Via Salaria Km. 29.5, C.P.10, I-00016 Monterotondo Stazione (Roma), Italy. E-mail: carlo@mlib.cnr.it*
[c] *Department of Chemistry, Faculty of Sciences, University of Assiut, Assiut, Egypt*

Received 19th April 2000, Accepted 23rd June 2000
First published as an Advance Article on the web 9th October 2000

The complexes $Fe[CH_3PO_3]\cdot H_2O$, $Fe_2[O_3P(CH_2)_2PO_3]\cdot 2H_2O$ and $Fe_2[O_3P(CH_2)_2PO_3]$ were synthesized and characterized by thermogravimetric analysis and UV-visible and infrared spectroscopy and their magnetic properties studied using a superconducting quantum interference device magnetometer. Preliminary X-ray single-crystal data suggest for $Fe[CH_3PO_3]\cdot H_2O$ a lamellar structure similar to that observed in $Cd[CH_3PO_3]\cdot H_2O$. The structure of cadmium phosphonate consists of alternating inorganic and organic layers, with the metal ion octahedrally coordinated by five oxygens from phosphonate and one from a water molecule. The inorganic layers are then separated by bilayers of methyl groups, and van der Waals contacts are established between them. In $Fe_2[O_3P(CH_2)_2PO_3]\cdot 2H_2O$ a pillared structure similar to that found in the corresponding zinc(II) ethylenebis(phosphonates) is suggested. All the compounds reported contain Fe^{II} in the d^6 ($S = 2$) high-spin electronic configuration, as determined from magnetic measurements in the high temperature region. Below 100 K the effective magnetic moment of $Fe[CH_3PO_3]\cdot H_2O$ decreases down to 30 K, then rises rapidly to a maximum at 24 K, and decreases again. The 3-D long-range antiferromagnetic order, defined as the temperature of the onset of the magnetization, has been located at $T_N = 25$ K. Similar behavior has been observed in $Fe_2[O_3P(CH_2)_2PO_3]\cdot 2H_2O$. Below the critical temperature, T_N, both compounds behave as a "weak ferromagnet". After dehydration $Fe_2[O_3P(CH_2)_2PO_3]\cdot 2H_2O$ loses the water molecules, and its magnetic behavior changes drastically in the low temperature region. The magnetic data at low temperatures of anhydrous $Fe_2[O_3P(CH_2)_2PO_3]$ are consistent with a magnetically disordered ground state, possibly a spin-glass like state.

Introduction

Hybrid layered compounds, consisting of alternating inorganic and organic layers, have provided interesting examples of low-dimensional magnetic materials.[1] Typical examples are the "*intercalation*"[2] and "*molecular composite*"[3] compounds. In contrast with intercalation compounds, where the organic molecules between layers of the inorganic lattice form only van der Waals interactions, in "molecular composite" solids the organic molecules are covalently or ionically bound to the inorganic layers. Further, the stoichiometric ratio of the host to guest in the intercalation compounds may vary, while in the molecular composite ones it is fixed by the requirements of the covalent or ionic bonding. The bonding causes also another effect: it fixes the orientation of the ligand in the lattice, thus giving often fully ordered crystals. An interesting class of "*magnetic molecular composite*" solids is represented by the transition metal(II) phosphonates, $M[RPO_3]\cdot H_2O$,[4] and metal(II) diphosphonates, $M_2[O_3P–R–PO_3]\cdot 2H_2O$[5,6] (M = Mn^{II}, Cr^{II}, Fe^{II}, Co^{II} or Ni^{II}; R = alkyl or aryl group). In the most common crystal structure, see Scheme 1, the metal ions are bridged by the oxygens of the phosphonate ligands and form sheets that are separated one from the other by the organic substituents of the ligands. The two-dimensional nature of the lattice favours next-neighbour exchange magnetic interactions in phosphonates containing paramagnetic ions and, at low temperatures, a long-range magnetic ordering is often observed. We have recently prepared $Fe_2[O_3P(CH_2)_nPO_3]\cdot 2H_2O$, $n = 1$ or 2,[7] $Fe[C_6H_5PO_3]\cdot H_2O$,[8] and $Cr[CH_3PO_3]\cdot H_2O$[9] and found

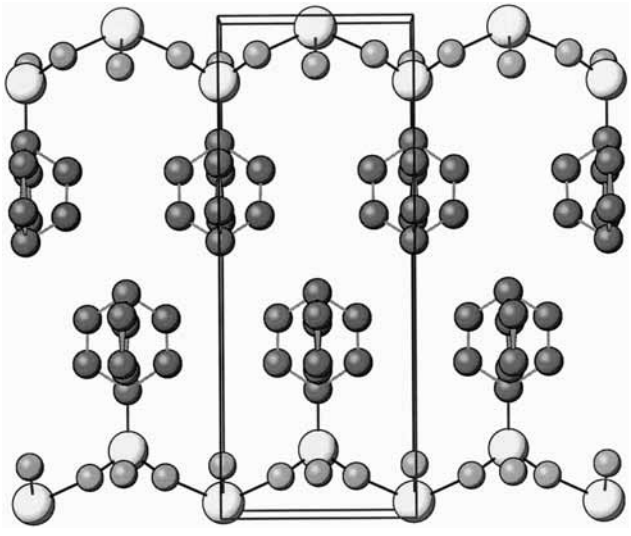

Scheme 1

† Based on the presentation given at Dalton Discussion No. 3, 9–11th September 2000, University of Bologna, Italy.

This journal is © The Royal Society of Chemistry 2000

that these compounds order antiferromagnetically at low temperatures. Below the antiferromagnetic ordering temperature, T_N, the equilibrium distribution of moments is not perfectly antiparallel, as is expected for an antiferromagnet, but canted from the magnetic easy-axis, giving rise to a spontaneous magnetization. The existence of a hysteresis loop, below the critical temperature, T_N, confers a memory effect on the material. This phenomenon is better known as *canted antiferromagnetism* or *weak ferromagnetism* and was observed for the first time in α-Fe_2O_3.[10]

This paper reports on the characterization and magnetic behavior at low temperatures of three new iron(II) organophosphonates, $Fe[CH_3PO_3]\cdot H_2O$, $Fe_2[O_3P(CH_2)_2PO_3]\cdot 2H_2O$ and anhydrous $Fe_2[O_3P(CH_2)_2PO_3]$. A brief communication of the synthesis and of the magnetic properties of $Fe_2[O_3P(CH_2)_2PO_3]\cdot 2H_2O$ has been presented earlier.[7]

Experimental

Materials and methods

Methylphosphonic acid, $CH_3PO_3H_2$, and ethylenediphosphonic acid $H_2O_3P(CH_2)_2PO_3H_2$ were of analytical grade (Aldrich Chemical Co.) used without further purification. HPLC water was used as solvent. All reactions involving iron(II) ion were carried out under an inert atmosphere by using the usual Schlenk techniques.

Synthesis of $Fe[CH_3PO_3]\cdot H_2O$

$FeSO_4\cdot 7H_2O$ (7 g, 25.18 mmol) was dissolved in 30 mL of water. The solution was filtered and added to a clean aqueous solution containing methylphosphonic acid (2.70 g, 28.12 mmol) and urea (3.00 g, 50 mmol). The resulting colourless solution was heated under nitrogen for a week at 90 °C. A white-grey microcrystalline powder (needle-like) separated from the solution was washed with water and dried under vacuum at room temperature. The compound is stable to the air. Calc. for $Fe[CH_3PO_3]\cdot H_2O$: C, 7.15; H, 3.00; Fe, 33.27; P, 18.45. Found: C, 7.18; H, 2.97; Fe, 34.05; P, 17.37%.

The synthesis of $Fe_2[O_3P(CH_2)_2PO_3]\cdot 2H_2O$ has been reported previously.[7] Both the iron(II) phosphonates are air-stable white polycrystalline compounds. Anhydrous $Fe_2[O_3P(CH_2)_2PO_3]$ was obtained by heating the corresponding hydrated salt under vacuum at $T \approx 300$ °C for several hours. The sample was stored under nitrogen because it absorbs water when exposed to the air. Elemental analyses were performed by Malissa and Reuter Mikroanalytische Laboratorien, Elbach, Germany. Thermogravimetric (TGA) data were collected in flowing dry N_2, at a rate of 5 °C min^{-1} on a Stanton-Redcroft STA-781 thermoanalyzer. The IR absorption spectra were obtained on a Perkin-Elmer 621 spectrophotometer by the KBr pellet and Nujol mull methods. Static magnetic susceptibility measurements were performed by using a Quantum Design MPMS5 SQUID susceptometer in fields up to 5 Tesla. A cellulose capsule was filled with freshly prepared polycrystalline sample and placed inside a polyethylene straw fixed to the end of the sample rod. All the experimental data were corrected for the core magnetization using Pascal's constants. Room temperature X-ray powder diffraction data were recorded on a Seifert XRD-3000 diffractometer, with a curved graphite single-crystal monochromator [λ(Cu-Kα) = 1.54056 Å] and a position sensitive detector operating in constant scan mode. The data were collected with a step size of 2θ 0.02° and at count time of 4 s per step of 0.2° min^{-1} over the range $4 < 2\theta < 80°$. The sample was mounted on a flat plate, giving rise to a strong preferred orientation. The diffractometer zero point was determined from an external silicon standard. The powder patterns were indexed by using a Seifert indexing program.

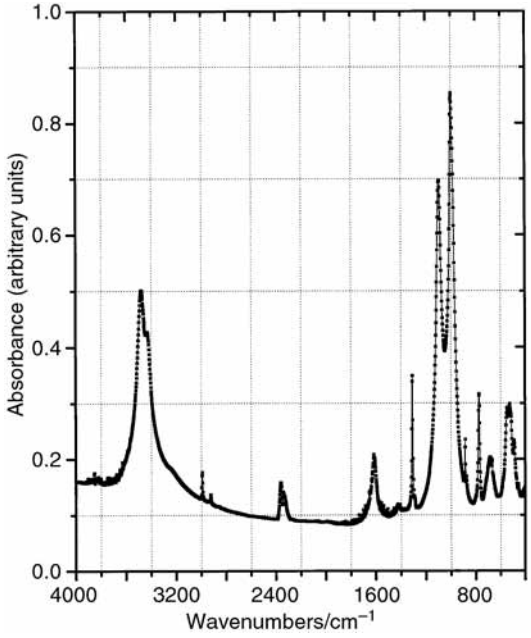

Fig. 1 Absorption FTIR spectrum of $Fe[CH_3PO_3]\cdot H_2O$ in the KBr region.

Results

Iron(II) phosphonates were prepared from the reaction of $FeSO_4\cdot 7H_2O$ with the appropriate acid in water, in the presence of urea at temperatures slightly above 80 °C, under an inert atmosphere. Under these conditions urea decomposes to give $(NH_4)_2CO_3$, thus increasing the pH of the solution. The compounds precipitated as white to light-grey microcrystalline powders after days of reflux. The final pH of the solution was found to be around neutral. Our method is general and was tested for several iron(II) and chromium(II) organophosphonates.[7–9] The compounds were characterized by elemental analyses, TGA, XRD techniques and IR spectroscopy.

Preliminary X-ray single-crystal data of $Fe[CH_3PO_3]\cdot H_2O$ suggest that the compound crystallizes in the orthorhombic space group $Pna2_1$, with the following unit-cell parameters: $a = 17.538(1)$, $b = 4.814(1)$, $c = 5.719(1)$ Å.[11] The compound is isomorphous with the layered $Cd[CH_3PO_3]\cdot H_2O$.[12] In this space group the interlayer direction is along the a axis. The TGA of $Fe[CH_3PO_3]\cdot H_2O$ shows one mass loss. It begins to lose co-ordinated water molecules at 150 °C ending at ≈290 °C. The observed weight loss at this stage is 10.52%, a value which corresponds to one water molecule per formula unit. After dehydration there is a weight loss above 500 °C, which can be ascribed to the decomposition of the ligand. The X-ray powder diffraction pattern of $Fe_2[O_3P(CH_2)_2PO_3]\cdot 2H_2O$ has been indexed in the monoclinic system, with the following unit-cell parameters: $a = 5.67(1)$, $b = 15.23(1)$, $c = 4.82(1)$ Å and $\beta = 90.4(1)°$. The TGA of $Fe_2[O_3P(CH_2)_2PO_3]\cdot 2H_2O$ shows one mass loss. The compound starts to lose co-ordinated water molecules at 220 °C ending at 320 °C. The observed weight loss at this stage is 9.34%, close to the calculated value, *i.e.* 10%, for two water molecules per formula unit. After dehydration, the weight loss of ≈5% observed above 500 °C corresponds to removal of the organic moieties. The compound remains crystalline after dehydration, as suggested from the XRD of $Fe_2[O_3P(CH_2)_2PO_3]$.

The IR spectra of $Fe[CH_3PO_3]\cdot H_2O$ and $Fe_2[O_3P(CH_2)_2PO_3]\cdot 2H_2O$ are reported in Figs. 1 and 2. They are similar and feature two intense bands, centered at 3420 and 3470 cm^{-1}, assigned as O–H stretching vibrations of co-ordinated water molecules. The strong and sharp nature of these bands indicates that the water is co-ordinated. The band observed at 1610 m

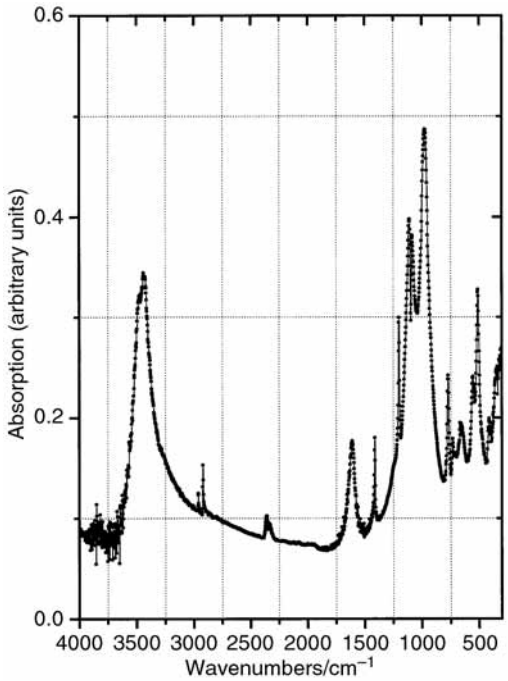

Fig. 2 Absorption FTIR spectrum of $Fe_2[O_3P(CH_2)_2PO_3]\cdot 2H_2O$ in the KBr region.

cm^{-1}, is assigned to the H_2O bending vibration. Four bands due to PO_3 group vibrations are observed in the range 1200–970 cm^{-1}. The complete conversion of the acid into the iron(II) salt is demonstrated by the absence of the OH stretching of POH at ≈2700–2550 and 2350–2100 cm^{-1}. Two small overtones at 2923 and 2970 cm^{-1} are due to the CH_2 group of the ligand. The IR spectrum of the dehydrated $Fe_2[O_3P(CH_2)_2PO_3]$ has also been recorded, and features the disappearance of the two intense bands 3420 and 3470 cm^{-1}, as well as that at 1610 cm^{-1}, all due to the vibrations of the co-ordinated water molecules.

Magnetic properties

$Fe[CH_3PO_3]\cdot H_2O$. Static magnetic susceptibility measurements were made on a polycrystalline sample with an applied field of 50 Oe from 5 to 260 K, by a SQUID magnetometer. The temperature dependence of the molar magnetic susceptibility, plotted as $1/\chi$ *vs.* temperature, is reported in Fig. 3. The plot is linear above 140 K, thus following the Curie–Weiss law. The fit to the data at temperatures above 140 K gave C 3.99 cm^3 K mol^{-1} and θ −59 K. The value of C corresponds to an effective magnetic moment of 5.65 μ_B, a value which is higher than that expected for spin-only Fe^{II}, d^6 ($S = 2$), in the high-spin electronic configuration, *i.e.* 4.9 μ_B. The free-ion ground state of Fe^{2+} d^6 ($S = 2$) is ^5D ($L = 2$), and the ion has orbital degeneracy. In a cubic ligand field the $^5T_{2g}$ ground term retains an orbital contribution to the total moment, so that the lowest spin–orbit state has $J = 1$. The introduction of a distortion in the FeO_6 site by the ligands causes a further splitting of the $J = 1$ state, and the resulting ground state can be either a singlet, $M_j = 0$, or doublet, $M_j = \pm 1$.[13] Since the energy separation between the spin-orbit components in Fe^{II} is of the order of 200 cm^{-1}, an orbital contribution to the moment is expected, and this could explain the observed difference between the measured effective magnetic moment and the spin-only value. The large negative value of θ indicates strong antiferromagnetic interactions between the nearest-neighbour magnetic ions. Below 25 K the product χT starts to increase and reaches a maximum at 24 K and then decreases again to 5 K, the lowest measured temperature. The temperature dependences of the zero-field-cooled (z.f.c.) magnetization and field-cooled (f.c.) magnetization were measured with an applied field of 50 Oe, and the plots

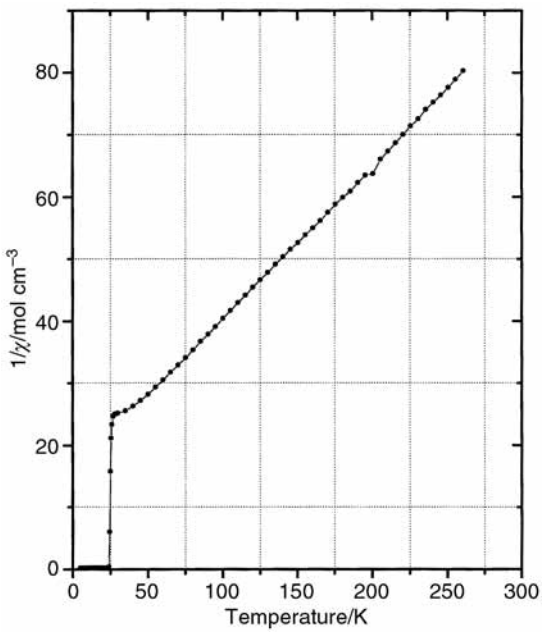

Fig. 3 $1/\chi$ *vs.* T plot of $Fe[CH_3PO_3]\cdot H_2O$ in the temperature range 5–260 K.

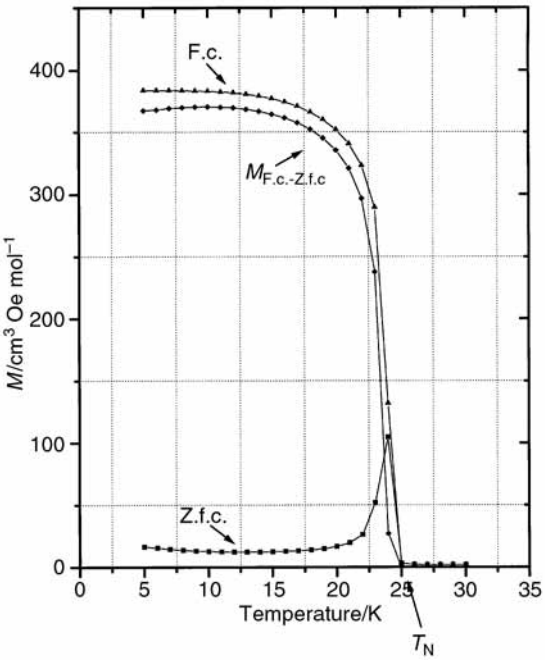

Fig. 4 *M vs. T* plot of $Fe[CH_3PO_3]\cdot H_2O$ in the temperature range 5–35 K in zero-field (■) and field cooling (▲) modes. (◆), Irreversible magnetization, as obtained from the difference of the f.c. and z.f.c. plots.

are shown in Fig. 4. A sharp increase of magnetization in the z.f.c. plot is observed at $T = 25$ K until the peak at 24 K is reached, while in the f.c. plot the magnetization increases up to 13 K and then remains constant down to 5 K. The temperature of onset of magnetization in the z.f.c. plot is taken as the Nèel temperature, T_N, *i.e.* 25 K. The difference between the f.c. magnetization and z.f.c. magnetization, $\Delta M_{fc\text{-}zfc}$, represents the irreversible magnetization, and is shown in Fig. 4. Below T_N the irreversible magnetization increases and begins to level off as the temperature approaches 5 K. The non-zero magnetization below T_N is evidence of a transition to a long-range magnetic order with spontaneous magnetization, and is consistent with a transition to a "canted antiferromagnetic" state. A hysteresis loop measured at a temperature near to that corresponding to the maximum in the z.f.c. plot, *i.e.* at 23 K, is reported in Fig. 5. The coercive field, H_{cM}, and the remnant magnetization,

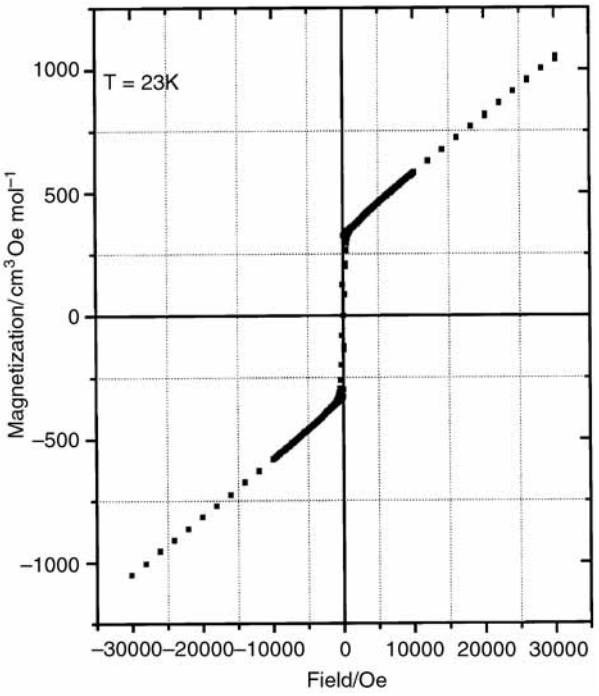

Fig. 5 Hysteresis loop of $Fe[CH_3PO_3]\cdot H_2O$ measured at 23 K.

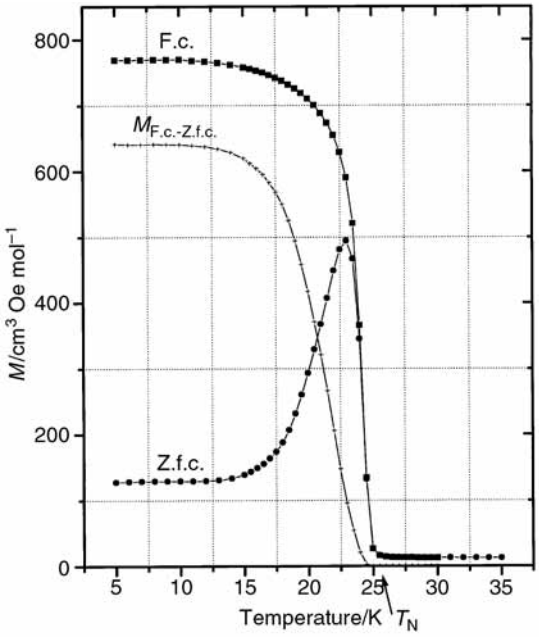

Fig. 6 *M vs.* T plot of $Fe_2[O_3P(CH_2)_2PO_3]\cdot 2H_2O$ in the temperature range 5–35 K in zero-field (●) and field cooling (■) modes. (+), Irreversible magnetization, as obtained from the difference of the f.c. and z.f.c. plots.

M_{remn}, were found to be 180 Oe and 325 cm^3 Oe mol^{-1}, respectively. The plot shows also that the magnetization consists of two contributions: $M = M_{nc} + \chi_{AFM}H$, where M_{nc} is the uncompensated (weak ferromagnetic) moment and χ_{AFM} is the antiferromagnetic susceptibility at that temperature. M_{nc} was obtained from the extrapolation to zero field of the linear part of the magnetization curve at high fields and χ_{AFM} was determined as its slope. The values were 350 cm^3 Oe mol^{-1} and 0.0235 cm^3 K mol^{-1}, respectively.

$Fe_2[O_3P(CH_2)_2PO_3]\cdot 2H_2O$. Static magnetic susceptibility measurements were made on a polycrystalline sample in a field of 50 Oe from 5 to 270 K, by a SQUID magnetometer. The sample was zero-field cooled to 5 K and the magnetization measured on heating to 270 K. The temperature dependence of the reciprocal of the molar magnetic susceptibility, $1/\chi$, is linear above 140 K and follows the Curie–Weiss law. The Curie constant, C, is 6.768 cm^3 K mol^{-1}, from a fit of the high temperature susceptibility data by using the equation $\chi = C/(T - \theta)$, and corresponds to an effective magnetic moment of 5.20 μ_B per Fe, consistent with the presence of Fe^{II} in a d^6 ($S = 2$) high-spin configuration. The large negative value of the Weiss constant, *i.e.* $\theta = -52$ K, indicates strong antiferromagnetic *near*-neighbour exchange between the adjacent iron(II) ions. Deviation from Curie–Weiss occurs below 80 K. The χT *vs.* T plot shows in fact a peak at ≈24 K. The temperature dependences of the z.f.c. and f.c. magnetization plots, measured with an applied field of 200 Oe, are shown in Fig. 6. The z.f.c. plot shows the onset at 25.0 K, which can be associated to the critical temperature, T_N. Below T_N the irreversible magnetization, $\Delta M_{fc\text{-}zfc}$, obtained as described above, increases and reaches a plateau at temperatures below 13 K. The magnetic hysteresis loop at 20 K was also measured, and the values of the coercive field, H_{cM}, and the remnant magnetization, M_{remn} were found to be 750 Oe and 1100 cm^3 Oe mol^{-1}, respectively, see Fig. 7. The latter value is ≈6% of the saturation value expected from an $S = 2$ spin system, as calculated from the relation $M_s = Ng\mu_B S$, where N is the Avogadro number. The isothermal M *vs.* H plot shows also that magnetization increases rapidly at low magnetic field and then with a linear dependence at larger applied magnetic fields, according to the previously reported relation: $M = M_{nc} + \chi_{AFM}H$. The fit to

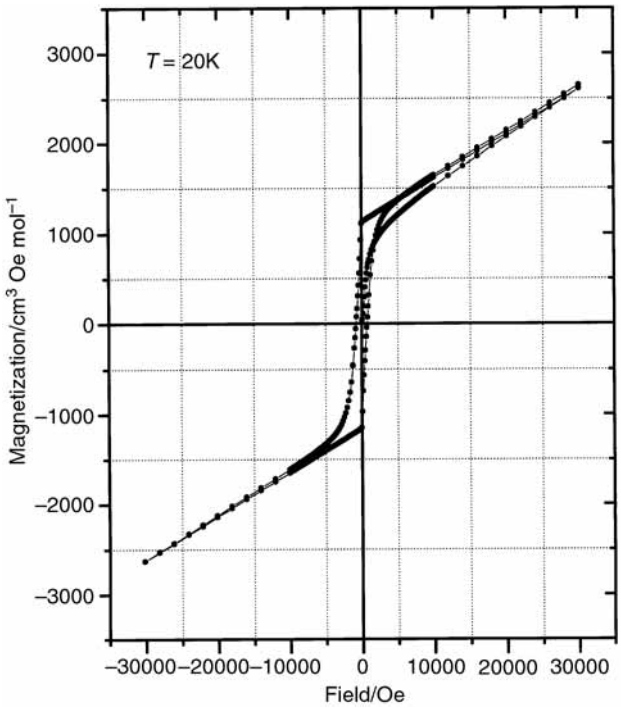

Fig. 7 Hysteresis loop of $Fe_2[O_3P(CH_2)_2PO_3]\cdot 2H_2O$ measured at 20 K.

the data gave the following values of M_{nc} and of χ_{AFM}: 1125 cm^3 Oe mol^{-1} and 0.0496 cm^3 K mol^{-1}.

$Fe_2[O_3P(CH_2)_2PO_3]$. Static magnetic susceptibility measurements of the anhydrous compound were made in the temperature range 5 to 280 K. It was zero-field cooled to 5 K and the magnetization measured on heating to 280 K. The reciprocal of the molar magnetic susceptibility, as a function of temperature is linear above 150 K and follows the Curie–Weiss law (see Fig. 8). The Curie constant is 5.65 cm^3 K mol^{-1}, from a fit to the high temperature susceptibility data using the equation $\chi = C/(T - \theta)$, and this corresponds to an effective magnetic moment of 4.8 μ_B per Fe, again consistent with the presence

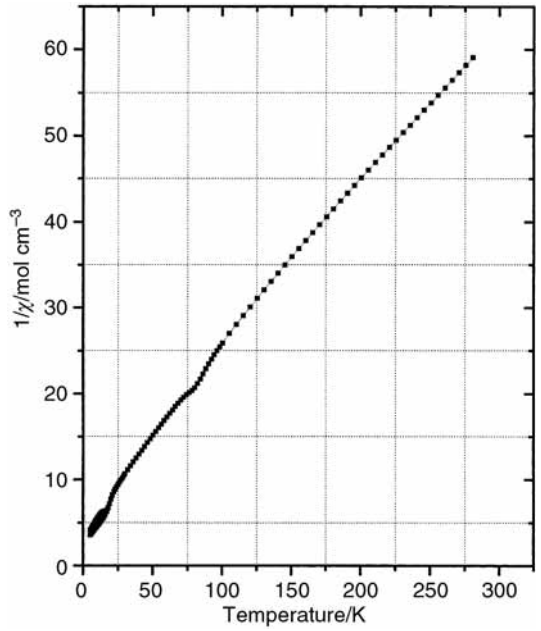

Fig. 8 $1/\chi$ *vs.* T plot of $Fe_2[O_3P(CH_2)_2PO_3]$ in the temperature range 5–275 K.

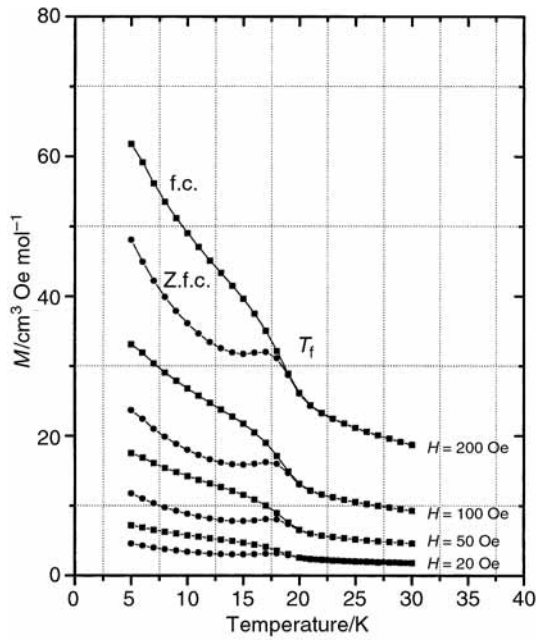

Fig. 9 *M vs. T* plot of $Fe_2[O_3P(CH_2)_2PO_3]$ in the temperature range 5–30 K, in zero-field (●) and field cooling (■) modes and at different applied fields.

of Fe^{II} in a d^6 ($S = 2$) high-spin configuration. The large negative value of the Weiss constant, *i.e.* $\theta = -53$ K, indicates strong antiferromagnetic *near*-neighbour exchange between the adjacent iron(II) ions. Deviation from Curie–Weiss occurs below 120 K. In the $1/\chi$ *vs.* T plot a small broad peak is observed at 75 K and another more pronounced one at 18 K. Z.f.c and f.c. magnetization *vs.* temperature experiments were performed at different fields in the temperature range 5 to 30 K, and are shown in Fig. 9. What it is observed below $T_{max} = 18$ K is that the z.f.c. magnetization deviates from the f.c. magnetization, indicating a dependence on the cooling procedure. A magnetization loop was also measured at 5 K and values of a coercive field, H_{cM}, and a remnant magnetization, M_{remn}, were found to be 70 Oe and 20 cm^3 Oe mol^{-1}, respectively (see Fig. 10 and inset). Further, an experiment on the time decay of the thermal remanent magnetization was also performed (see

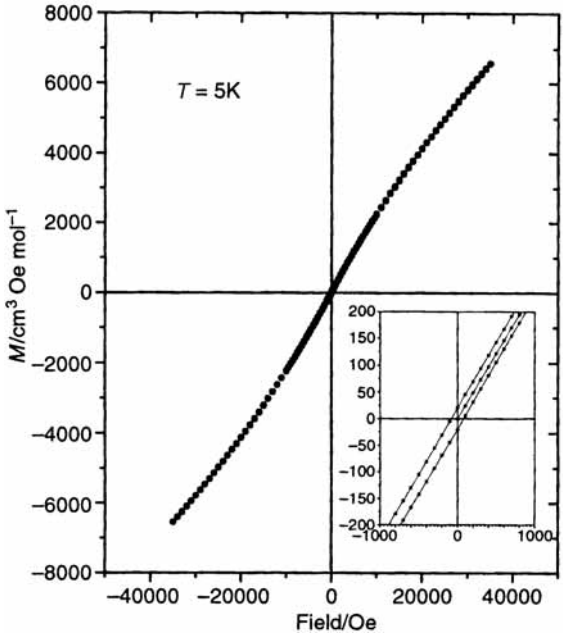

Fig. 10 Magnetization loop of $Fe_2[O_3P(CH_2)_2PO_3]$ measured at 5 K. The inset shows the hysteresis behavior in the low field region.

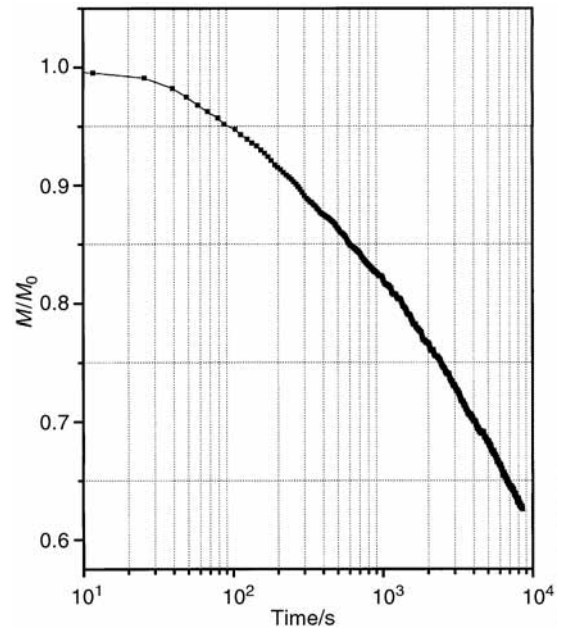

Fig. 11 A plot of the thermal remanent magnetization as a function of time for $Fe_2[O_3P(CH_2)_2PO_3]$.

Fig. 11). The sample was field-cooled in an external field of 100 Oe down to 5 K and then, after the applied field was switched off, the remanent magnetization was measured as function of time. This process induces in the paramagnetic region a partial alignment of the spins, which are frozen on cooling. Below T_{max} the field was removed but, since the spins are frozen, *i.e.* their alignment is not quenched, a net moment is present in the material. The decay of the thermal remanent magnetization is not logarithmic, as can be seen in Fig. 11. After 140 minutes the remnant magnetization is reduced by 40%. The existence of the relaxation phenomena is an indication of the presence of metastable magnetic states, among which the system evolves in time. However, the observed increase of the z.f.c. magnetization in the *M vs. T* plot below 12 K suggest the coexistence of a fraction of unfrozen spins or small clusters. These data are consistent with the existence of a disordered magnetic ground state, possibly spin-glass like.[14,15]

Table 1 Magnetic parameters of iron(II) phosphonates

Compound	T_N/K	θ/K	T_N/θ	Space group	Interlayer distance/Å	Ref.
$(NH_4)FePO_4 \cdot H_2O$	26.0	−65	0.40	$Pmn2_1$	8.8213(2)	22
$Fe[CH_3PO_3] \cdot H_2O$	25.0	−59	0.42	$Pna2_1$	8.81	This work
$Fe[C_2H_5PO_3] \cdot H_2O$	24.5	−43	0.57	$P1n1$	10.33(1)	13
$Fe[C_6H_5PO_3] \cdot H_2O$	21.5	−56	0.38	$Pmn2_1$	14.453(2)	9
$Fe[O_3P(CH_2)_2PO_3] \cdot 2H_2O$	25.0	−52	0.48		15.23	This work

Conclusion

Two weak ferromagnetic iron(II) organophosphonates have been prepared under an inert atmosphere and characterized. When isolated, the compounds are stable to the air. In both compounds the Fe^{II} is six-co-ordinated by five oxygen atoms of the phosphonate ligand and one from a water molecule and the electronic configuration is d^6 ($S = 2$) high-spin. From preliminary X-ray single-crystal data it is quite likely that $Fe[CH_3PO_3] \cdot H_2O$ will have the same layered structure observed in $Cd[CH_3PO_3] \cdot H_2O$,[12] $Fe[C_2H_5PO_3] \cdot H_2O$[16] and in $Fe[C_6H_5PO_3] \cdot H_2O$ and that $Fe_2[O_3P(CH_2)_2PO_3] \cdot 2H_2O$ should have a pillared structure, similar to that observed in the zinc(II) analogue.[17] $Cd[CH_3PO_3] \cdot H_2O$, for example, crystallizes in the orthorhombic space group $Pna2_1$, with unit-cell parameters a = 17.763(6), b = 5.008(2), c = 5.912(3) Å, $Z = 4$.[12] It shows a lamellar structure, consisting of roughly coplanar layers of cadmium atoms, co-ordinated octahedrally by five phosphonate oxygen atoms and one water molecule. These layers are then separated along the a axis by bilayers of the methyl groups, thus giving an alternation of organic and inorganic layers along the direction perpendicular to the inorganic planes. When the water molecule is removed from the pillared $Fe_2[O_3P(CH_2)_2PO_3] \cdot 2H_2O$ salt the grey powdered anhydrous salt remains crystalline. The compounds reported in this work, except for the anhydrous one, order antiferromagnetically at $T_N = 25$ K, and the antiferromagnetism arises from interactions between nearest neighbor ions that take place *via* two different 180° Fe–O–Fe superexchange paths. The values of $|T_N/\theta|$ observed are ≈0.4 (see Table 1), and this is consistent with the presence of a layered structure. In fact, molecular field predicts $|T_N/\theta| = 1$, and large deviations are expected for low-dimensional magnets because of the short-range correlations above the critical temperature. Below T_N the observed weak ferromagnetism is due to *spin canting*.[18,19] In this situation the local spins in the ordered magnetic state are not perfectly antiparallel, which results in an uncompensated resultant moment in one direction. Two mechanisms have been suggested for producing spin canting. The first is the single-ion magnetocrystalline anisotropy energy, which results when there are two equivalent sites of magnetic ions, but the directions of their anisotropy axes are different, and this is the case of NiF_2.[18] The second mechanism is known as the antisymmetric exchange, and it is a combined effect of the spin–orbit coupling and of the isotropic superexchange interactions. This type of exchange, which operates in addition to the isotropic Heisenberg exchange, is described on a microscopic level as $H_{aniso} = \boldsymbol{d}[\boldsymbol{S}_1\boldsymbol{S}_2]$, where $\boldsymbol{d}$ is a constant vector that depends on the symmetry of the crystal. The coupling acts to cant the spins, because the coupling energy is minimized when the two spins are perpendicular to each other. The antisymmetric exchange derives from the anisotropic spin interaction, which can be described as a sum of symmetric and antisymmetric components[19] $V_{1,2} = \boldsymbol{s}_1\boldsymbol{K}_S\boldsymbol{s}_2 + \boldsymbol{s}_1\boldsymbol{K}_A\boldsymbol{s}_2$, where the two tensors $\boldsymbol{K}_S$ and $\boldsymbol{K}_A$ are approximated as: $K_s \approx (\lambda/\Delta)^2 J \approx (\Delta g/g)^2 J$ and $K_A \approx (\lambda/\Delta)J \approx (\Delta g/g)J$, and λ is the spin–orbit coupling, Δ the ligand field splitting, and $\Delta g = g - 2$. Since only the antisymmetric component can cause spin canting, the anisotropy in the g value is therefore required. Here, to a first approximation, the ground state of Fe^{2+} ion in an octahedral ligand field is $^5T_{2g}$ and the low-site symmetry present in the compounds induces the anisotropy of g, which it should then be responsible for the weak ferromagnetism in these iron(II) phosphonates. This mechanism has previously been proposed to explain the presence of spin canting in manganese(II) alkylphosphonates.[20] Molecule-based "*weak ferromagnets*"[8,9,16,20] represent another category of insulating magnetic solids, having a finite zero-field spontaneous magnetization. This state could be obtained by combining two effects: the easier tendency to order antiferromagnetically observed in magnetic insulators, with a low-symmetry site around the metal ions, obtained by using here phosphonate ligands as chelating agent in the formation of the compound. Finally, it is worth noticing that the critical temperatures observed in the iron(II) phosphonate series, see Table 1, appear to depend little on the interlayer spacing, similarly to what is observed in the manganese analogues[20] and in other layered magnetic materials.[21] Further studies are in progress to solve the crystal structures of the reported compounds, in an attempt to correlate the crystal structure and the magnetic properties, and, finally, for studying the nature of the magnetic disordered state observed in the anhydrous $Fe_2[O_3P(CH_2)_2PO_3]$ salt.

Acknowledgements

We acknowledge support from Consiglio Nazionale delle Ricerche (Italy) and the Academy of Scientific Research and Technology (Egypt). One of us (C. B.) would like also to thank Mr. F. Federici, Mr. P. Filaci, Mrs. C. Riccucci and Mr. C. Veroli and a Degree in Chemistry student, Mrs. Daniela Caschera, for the experiments and Dr. D. Fiorani for helpful discussions.

References

1 R. Navarro, in *Magnetic Properties of Layered Transition Metal Compounds*, ed. L. J. De Jongh, Kluwer Academic Publ., Dordrecht, 1990.
2 D. O'Hare, in *Inorganic Materials*, eds. D. W. Bruce and D. O'Hare, John-Wiley & Sons, New York, 1992, pp. 165–228.
3 P. Day, *Philos. Trans. R. Soc. London*, *Ser. A*, 1985, **314**, 145.
4 G. Alberti, in *Comprehensive Supramolecular Chemistry*, ed. J. M. Lehn, Pergamon Press, Oxford, 1996, vol. 7, p. 151.
5 A. Clearfield, *Prog. Inorg. Chem.*, 1998, **47**, 371.
6 G. Cao, H. Hong and T. E. Mallouck, *Acc. Chem. Res.*, 1992, **25**, 420.
7 C. Bellitto, F. Federici, S. A. Ibrahim and M. R. Mahmoud, *1998 MRS Fall Meetings Proc.*, 1999, **547**, 487.
8 C. Bellitto, F. Federici and S. A. Ibrahim, *Chem. Commun.*, 1996, 759.
9 C. Bellitto, F. Federici, A. Altomare, R. Rizzi and S. A. Ibrahim, *Inorg. Chem.*, 2000, **39**, 1803.
10 See for example: R. L. Carlin, *Magnetochemistry*, Springer-Verlag, Berlin, 1986, p. 149.
11 M. Colapietro, unpublished results.
12 G. Cao, V. M. Lynch and L. N. Yacullo, *Chem. Mater.*, 1993, **5**, 1000.
13 B. N. Figgis, *Introduction to Ligand Fields*, Interscience, London, 1966, p. 289.
14 K. Binder and A. P. Young, *Rev. Mod. Phys.*, 1986, **58**, 802.
15 R. V. Chamberlin, *J. Appl. Phys.*, 1985, **57**, 3377.

16 B. Bujoli, O. Pena, P. Palvadeau, J. Le Bideau, C. Payen and J. Rouxel, *Chem. Mater.*, 1993, **5**, 583; J. Le Bideau, C. Payen, B. Bujoli, P. Palvadeau and J. Rouxel, *J. Magn. Magn. Mater.*, 1995, **140**, 1719.
17 D. M. Poojary, B. Zhang and A. Clearfield, *J. Am. Chem. Soc.*, 1997, **119**, 12550.
18 T. Moriya, *Phys. Rev.*, 1960, **117**, 635
19 I. Dziyaloshinsky, *J. Phys. Chem. Solids*, 1958, **4**, 241; T. Moriya, *Phys. Rev.*, 1960, **120**, 91; T. Moriya in *Magnetism*, eds. G. T. Rado and H. Suhl, Academic Press, New York, 1966, vol. 1, p. 85.
20 S. Carling, P. Day, D. Visser and R. K. Kremer, *J. Solid State Chem.*, 1993, **106**, 111.
21 M. Kurmoo, *Chem. Mater.*, 1999, **11**, 3370.
22 J. E. Greedan, K. Reubeunbauer, T. Birchall and M. Ehlert, *J. Solid State Chem.*, 1988, **77**, 376.